JACS
JOURNAL OF THE AMERICAN CHEMICAL SOCIETY

ARTICLE

pubs.acs.org/JACS

Multicolor, One- and Two-Photon Imaging of Enzymatic Activities in Live Cells with Fluorescently Quenched Activity-Based Probes (qABPs)

Mingyu Hu,[†] Lin Li,[†] Hao Wu,[†] Ying Su,[†] Peng-Yu Yang,[†] Mahesh Uttamchandani,[†,‡] Qing-Hua Xu,[†] and Shao Q. Yao*[,†,§,∥]

[†]Department of Chemistry, [§]Department of Biological Sciences, and [∥]NUS MedChem Program of the Life Sciences Institute, National University of Singapore, Singapore 117543

[‡]Defence Medical and Environmental Research Institute, DSO National Laboratories, Singapore 117510

Supporting Information

ABSTRACT: Fluorescence imaging provides an indispensable way to locate and monitor biological targets within complex and dynamic intracellular environments. Of the various imaging agents currently available, small molecule-based probes provide a powerful tool for live cell imaging, primarily due to their desirable properties, including cell permeability (as a result of their smaller sizes), chemical tractability (e.g., different molecular structures/designs can be installed), and amenability to imaging a wide variety of biological events. With a few exceptions, most existing small molecule probes are however not suitable for *in vivo* bioimaging experiments in which high-resolution studies of enzyme activity and localization are necessary. In this article, we reported a new class of fluorescently Quenched Activity-Based Probes (qABPs) which are highly modular, and can sensitively image (through multiple enzyme turnovers leading to fluorescence signal amplification) different types of enzyme activities in live mammalian cells with good spatial and temporal resolution. We have also incorporated two-photon dyes into our modular probe design, enabling for the first time activity-based, fluorogenic two-photon imaging of enzyme activities. This, hence, expands the repertoire of 'smart', responsive probes currently available for live cell bioimaging experiments.

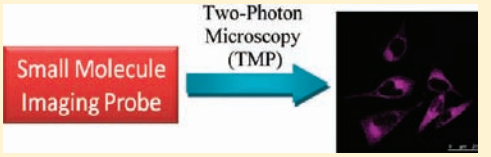

INTRODUCTION

Fluorescence imaging provides an indispensable way to locate and monitor biological targets within complex and dynamic intracellular environments.[1] The breadth of imaging experiments is arguably limited by the variety of detection probes available. Such imaging probes can report, in real-time, points within cells or tissues that exhibit intended interactions or activities, providing a detailed picture of biological processes that occur *in vivo*. In general, there are three classes of probes used for *in vivo* imaging experiments, namely, those based on fluorescent proteins (FPs),[1a−c] bioconjugated nanomaterials,[1d] and small molecules.[1e,f] Fluorescent proteins are genetically encoded, hence do not require external application and delivery. As macromolecular imaging probes, however, they have numerous shortcomings for intracellular applications.[2] For example, they may not distribute evenly in cells, provide sufficient handles for rational modification/design or deliver required sensitivities or specificities. Nanomaterials such as quantum dots obviate some of these problems by offering much improved sensitivities and other chemical and physical properties, but themselves are macromolecular in nature, therefore, offering limited solutions.[1e,f] Small molecule-based probes provide a powerful tool for live cell imaging, primarily due to their desirable properties, including cell permeability (as a result of their smaller sizes), chemical tractability (e.g., different molecular structures/designs can be installed), and amenability to imaging a wide variety of biological events.[2] In recent years, many research groups have successfully developed and deployed small molecule imaging probes for intracellular detection of ions, metabolites, proteins (including enzymes), organelles, and different types of cells/tissues.[1e,f,3−7] Of particular importance are small molecule-based probes capable of reporting *in vivo* enzymatic activities,[4−7] as few FP-based, enzyme-detecting biosensors are currently available and they suffer from limited dynamic range of detection and many other problems.[8] Most small molecule approaches make use of a cell-permeable reporter substrate that, upon being processed by an endogenous enzyme target, produces a fluorescence signal that can be visualized microscopically.[5] These probes, however, normally diffuse away from the site of reaction rapidly, thus, providing limited utilities in high-resolution studies of enzyme activity and localization.[6]

Several probe designs have begun to address this challenge of enabling smart, precise sensing of enzymatic activity *in vivo* (Figure 1).[4,7] The commercial product ELF 97 acts as a substrate for both acid and alkaline phosphatases, a group of highly regulated enzymes critical in modulating signal transduction pathways.[4] Upon enzymatic removal of the phosphate residue, the water-soluble substrate forms a bright yellow-green fluorescent product which precipitates at the site of enzymatic activity. This enables good spatial resolution of phosphatase activities in cells (Figure 1A). The strategy, however, is in general applicable

Received: February 4, 2011
Published: July 06, 2011

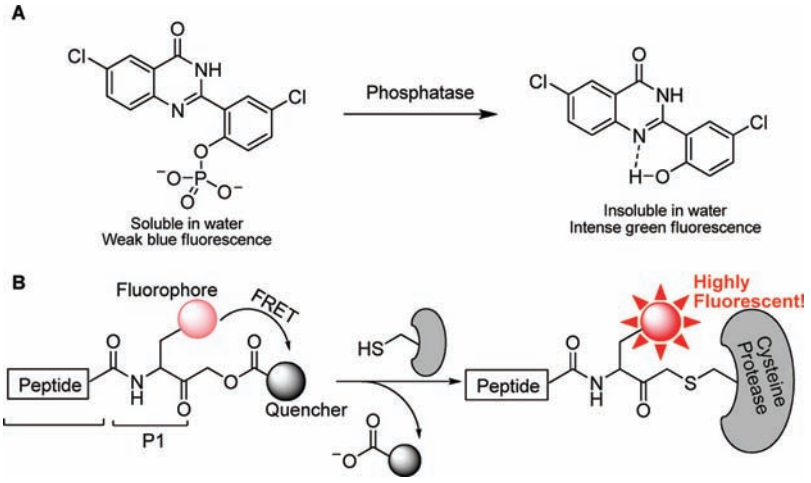

Figure 1. Two existing small molecule approaches for spatially resolved imaging of enzymatic activities *in vivo*. (A) ELF 97 phosphatase substrate.[4] (B) Acyloxymethyl ketone (AOMK)-based quenched activity-based probes (qABPs) liberate fluorescence upon proteolysis and covalently bind the enzyme at its active site.[7]

to phosphatases, although recent studies have indicated that, when coupled with clever linker design, it may be adaptable to the detection of proteases as well.[9] Bogyo and co-workers recently developed the so-called fluorescently quenched activity-based probes (qABPs) to monitor real-time protease activities in live human cells (Figure 1B).[7,10] By using acyloxymethyl ketone (AOMK)-based probes which emit a strong fluorescent signal only after proteolysis by a cysteine protease target, with the simultaneous formation of a covalent probe−enzyme adduct, this strategy couples imaging and suicide inhibition within the same design to achieve the intended "turn-on" imaging capability for cysteine proteases *in vivo* with good spatial resolution.[7] While highly elegant, this approach may suffer from some limitations. For example, the method was based on a suicide inhibitor which, unlike ELF 97, provided no signal amplification, thus, potentially obscuring the probe's ability to truly monitor enzyme activity and limiting its sensitivity when screening low-abundance targets. We would like to point out, however, in a recent study carried out to directly compare fluorescent ABPs and commercially available polymer-based substrates of proteases as imaging reagents, Bogyo and co-workers showed that their ABPs might offer similar or even better sensitivities, presumably due to more desirable cellular uptake and retention properties.[11]

Herein, based on the well-established quinone methide chemistry,[12−14] we have successfully developed a new class of fluorescently qABPs which are highly modular, and can sensitively image (through multiple enzyme turnovers leading to fluorescence signal amplification) different types of enzyme activities in live mammalian cells with good spatial and temporal resolution (Figure 2). We have also incorporated two-photon dyes into our modular probe design (vide infra),[3] enabling for the first time activity-based, fluorogenic two-photon imaging of enzyme activities. This, hence, expands the repertoire of 'smart', responsive probes currently available for live cell bioimaging experiments.[1−8]

RESULTS AND DISCUSSION

Design Principle of Quinone (or Quinolimine) Methide-Based qABPs. Quinone (or quinolimine) methide-based small molecule probes were previously used for *in vitro* labeling of enzymes either in their purified form, in cell extracts or recombinantly expressed inside bacterial cells.[13] It has been well-established that the diffusible nature of these probes causes the labeling to occur away from catalytic active site of the target enzyme.[14] Recent studies have further shown that release of the quinone methide intermediate from the active site of the target occurs at a rate competitive with the subsequent labeling process (i.e., Pathways A−C in Figure 2), causing nonspecific labeling of other proteins (and thus making them ill-suited for activity-based profiling of proteomes[15]).[12b] We exploited this unique feature to design the new class of qABPs suitable for *in vivo* bioimaging (Figure 2); these probes contained modular components, including an enzyme substrate warhead (**WH**), a fluorescence reporter and a quencher, strategically built around a mandelic acid core. Other tags such as biotin or CPP (cell-penetrating peptide) may be introduced as well, when needed.[16,17] The resulting fluorogenic probes were normally in the "off" state in which the reporter fluorescence was effectively quenched by the proximal Dabcyl quencher. Upon introduction into cells and enzymatic cleavage of the **WH**, an 1,6-elimination reaction led to the release of the quencher group, liberating fluorescence and a quinone/quinolimine methide intermediate. By taking advantage of the reactive yet diffusible nature of this intermediate, we were able to achieve both sufficient spatial resolution to 'image" enzyme localization, and fluorescence signal amplification to sensitively report endogenous multiturnover enzyme activity. We envisioned in a typical live cell imaging experiment, of the three pathways possible for the intermediate, Pathway C was the most productive (Figure 2A); a substantial amount of the quencher-released, highly fluorescent intermediate had a long enough half-life to diffuse out of the enzyme active site (thus keeping the bulk of the enzyme target unmodified for multiple catalytic conversions), and label available nucleophiles within its immediate vicinity (e.g., proteins residing in the same subcellular organelle as the intended target). Taking advantage of this property, fluorescence would be accumulated at the site of activity *in situ*, magnifying overall readouts. Furthermore, the design enabled different dyes (e.g., 1-P/2-P dyes), and substrate elements to be introduced as desired, in a modular fashion.

Chemical Synthesis of the Probes. To validate our new qABP design, six model probes (**P1**−**P6**) were synthesized and used to study two different classes of enzymes, namely, caspases

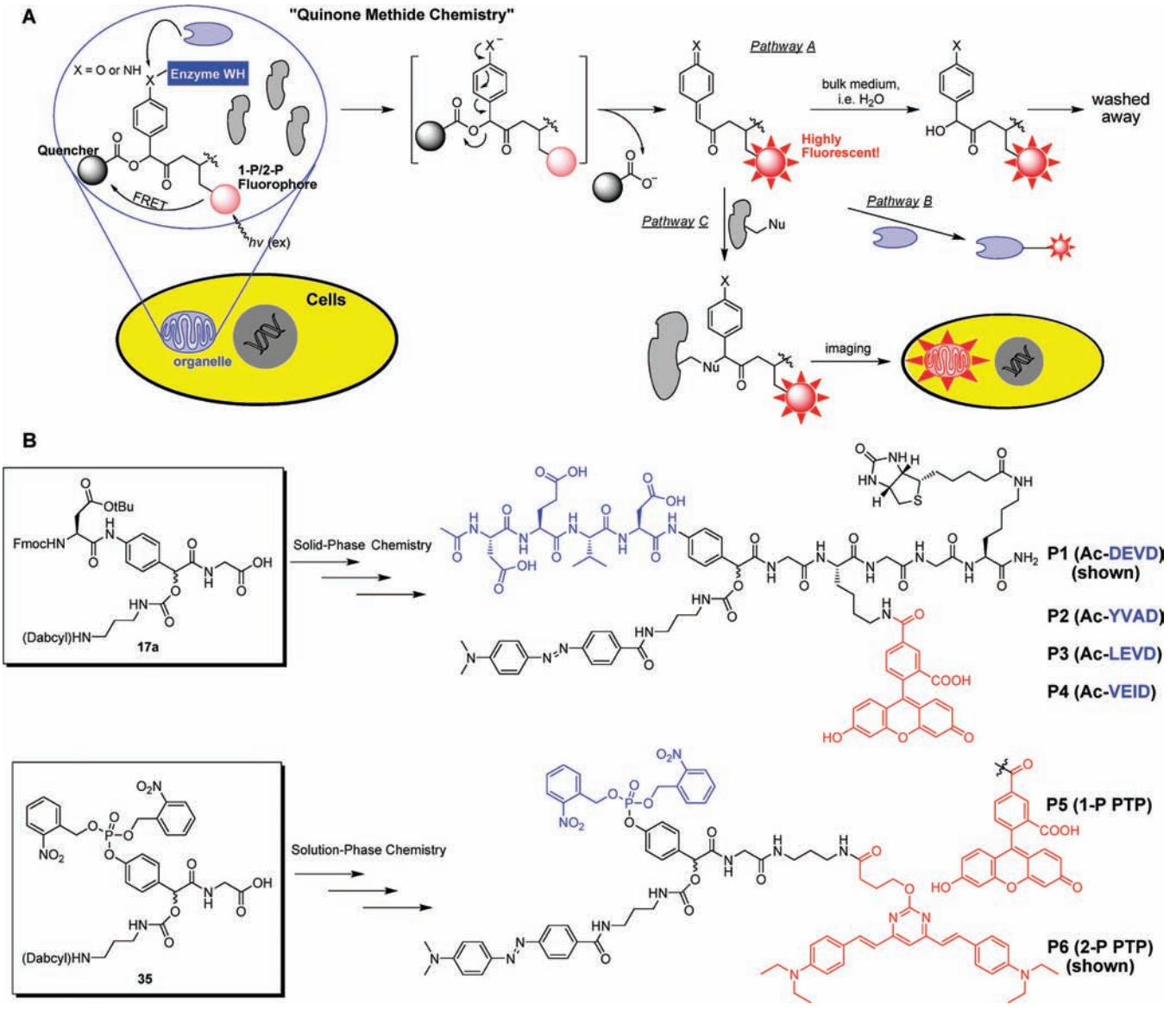

Figure 2. (A) Overall design principle of our quenched activity-based probes (qABPs). The probe includes three elements (or modules), specifically the fluorophore (in red), the quencher (and/or a tag like biotin), and an enzyme recognition warhead (**WH**; in blue) that surround a mandelic acid core. These modules are interchangeable, allowing the strategy to be broadly applicable to different types of enzymes. Upon cleavage of **WH** by the enzyme, the probe released the quencher, producing a reactive quinone (or quinolimine) methide intermediate (in bracket). In an intracellular environment, three pathways of this reactive intermediate are possible: (A) it is hydrated/quenched with bulk water; (B) it binds a nucleophile within the enzyme of interest but does not necessarily inactivate the enzyme; (C) it reacts with a nearby nucleophile and accumulates in the same organelle where the enzymatic reaction occurs. (B) Structures of probes (**P1**−**P6**) used in the current study. The strategy is demonstrated with, but not limited to, cysteine proteases (top) and phosphatases (bottom). Both one- and two-photon fluorophores were incorporated. Detailed synthetic schemes and procedures are provided in the Experimental Section and the Supporting Information.

(a clan CD cysteine protease subclass) and protein tyrosine phosphatases (PTPs) (Figure 2B). Two additional control probes, **C1** and **C2**, were also synthesized (Figure 3). It should be noted that the modularity of our probe design should enable this strategy to be readily applicable to most other hydrolytic enzymes (e.g., all four major classes of proteases[13b,c]). The synthesis of caspase probes **P1**−**P4** involved both solution- and solid-phase chemistry (Scheme S2 in the Supporting Information); from a commercially available starting material, compound **17a** was synthesized in 12 solution-phase steps. Briefly, the first three steps were modified from published procedures.[13c] Selective protection of the *tert*-butyl group thereafter yielded acid **9b** which was coupled with allyl-protected glycine to produce compound **11**. After hydrolysis of the acetyl group, the nitro group was reduced to amine and coupled with first amino acid, aspartic acid, to afford product **14**. The secondary alcohol was activated by *p*-nitrophenyl chloroformate and coupled with Dabcyl-containing amino linker to form the carbamate adduct **16**. The building block **17** was obtained by deprotection of allyl group using palladium catalyst. Finally, **P1**−**P4** (each containing a different substrate **WH**—DEVD, YVAD, LEVD, and VEID, respectively, targeting different classes of caspases[18]) were assembled by solid-phase peptide synthesis. A biotin tag was introduced for future pull-down/target

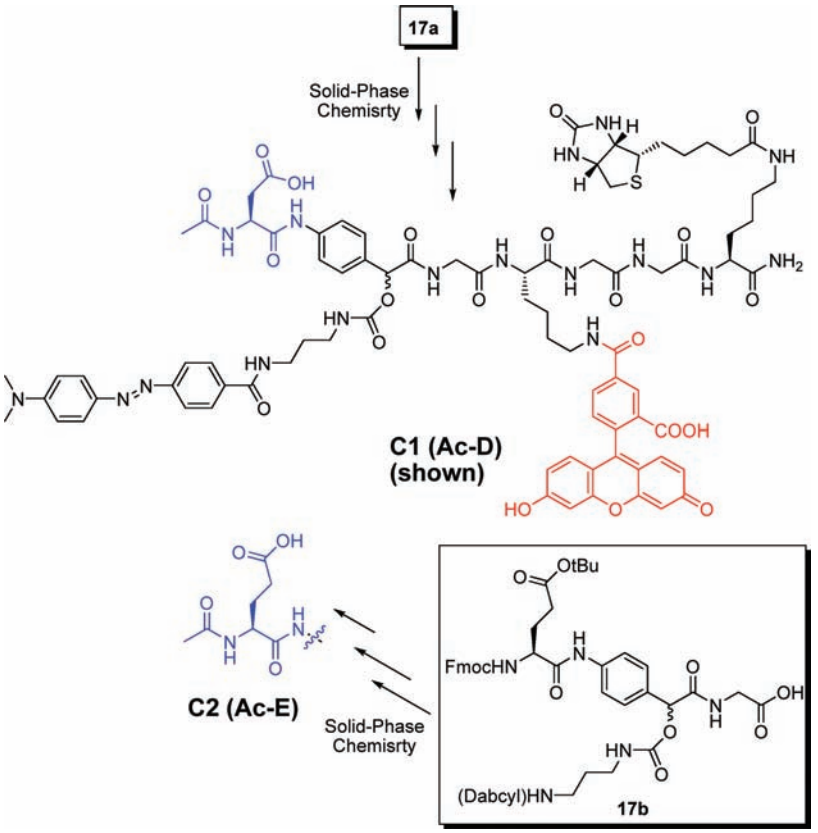

Figure 3. Structures of the two control probes **C1** and **C2**. Similar to Figure 2, of the three modular components in each probe that surround the mandelic acid core, the fluorophore and the enzyme recognition warhead (**WH**) were highlighted in red and blue, respectively. **WH** in **C1** and **C2** are acetylated Asp and Glu, respectively.

identification purposes, but may be replaced with a CPP when needed (vide infra).[17] After cleavage from resin, the crude products were further purified and fully characterized. The amenability of our synthetic strategy to solid-phase synthesis should allow easy access to other probes in the future. The PTP probes, **P5** and **P6**, were similarly synthesized on the mandelic acid core structure with solution-phase chemistry (Scheme S3). Instead of peptide-based substrates, a "caged" phosphate group was incorporated, followed by a two-step carbamation reaction to yield compound **34**. After deprotection of the allyl group, fluorescein and dye **22** (a two-photon dye) were directly coupled to give the final probes **P5** and **P6**, respectively. The "caging" of the phosphate in the two probes enabled temporal control of "imaging" PTP activities in live cells.[19] To minimize the size of these probes, biotin tag was omitted.

In previous studies by Bogyo and co-workers, where AOMK-containing activity-based probes were developed to target a variety of cysteine proteases including caspases, cathepsins, and legumain, the authors found that Asp-AOMK, a probe which contains a single aspartic acid residue at the P_1 position and was intended for caspases, cross-reacted readily with human legumain.[20] Legumain is a CD-clan lysosomal cysteine protease that plays a pivotal role in the endosomal/lysosomal degradation system. It specifically cleaves peptide bonds with Asn or Asp at the P_1 position.[21] To unambiguously confirm that our caspase-detecting probes, **P1**−**P4**, did not cross-react with other endogenous cysteine proteases especially legumain, **C1** and **C2** control probes, each containing a single acetylated Asp and Glu residue at the P_1 position, respectively, to make up the **WH** of the probes, were also designed (Figure 3). These two probes were similarly synthesized from the corresponding key intermediates, **17a** and **17b**, respectively.

Mechanistic Studies of the Probes with Recombinant Enzymes. The caspase probes **P1**−**P4**, together with the two control probes **C1** and **C2**, were first tested *in vitro* with several recombinant cysteine proteases, namely, caspases (1, 3, 4, 6, 7, 8 and 9), cathepsins (B, L and S), and legumain. The standard microplate-based enzymatic assay was adopted, and the fluorescence results after an 1-h incubation were plotted in Figure 4A. **P1** (Ac-DEVD) exhibited strong fluorescence readouts with caspase-3 and -7, with some cross-reactivity with caspase-6 and -8. **P2** (Ac-YVAD) was only recognized by caspase-1 and -4 which are both potential regulators of inflammation. **P3** (Ac-LEVD) and **P4** (Ac-VEID) mainly targeted caspase-1 and -4, and caspase-4 and -6, respectively. As intended, none of the four probes showed any cross-reactivity with recombinant cathepsins, the most abundant cysteine proteases in mammalian cells, nor did they cross-react with legumain. Interestingly, the two control probes, **C1** and **C2**, also showed no reactivity in our assay conditions against all enzymes tested, including legumain.[22] This is in sharp contrast to previous findings using the Asp-AOMK probe where significant cross-reactivity was observed.[20] While the exact reason for the discrepancy is still under our investigation, we believe it is caused by obvious intrinsic differences in the design of these two qABP systems and chemical structures of the probes. Our new qABPs thus worked as expected *in vitro*, and showed excellent substrate specificity toward intended enzyme targets (i.e., caspases).[18] Owing to the essential roles of caspase-3

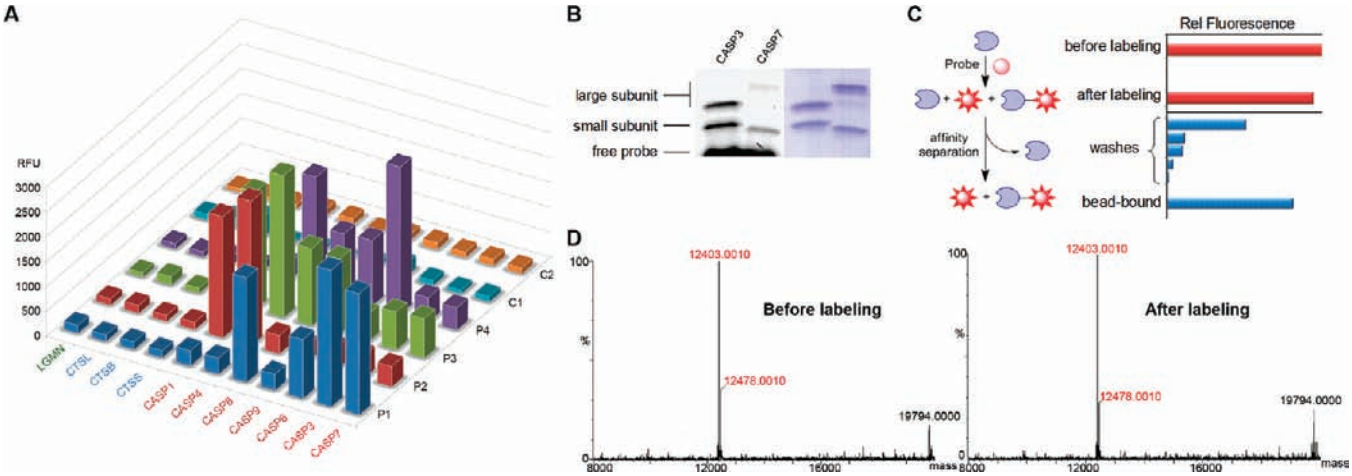

Figure 4. Mechanistic studies of **P1**−**P4**, together with control probes **C1** and **C2**, against recombinant enzymes. (A) Substrate specificities of all six probes (bottom to top: **P1**, **P2**, **P3**, **P4**, **C1**, **C2**) toward recombinant caspases, cathepsins, and legumain in a microplate-based enzyme assay. Left to right: legumain, cathepsins (L, B and S), and caspases (-1, -4, -8, -9, -6, -3 and -7). RF values were obtained after a 1-h incubation. Kinetic studies of **P1** against caspase-3 and -7 are shown in Figure S10 in the Supporting Information. (B) *In vitro* labeling of **P1** against purified capase-3 and -7. Free probe was observed in the dye front at the bottom of the gel. A small amount of the enzyme was labeled. (C) Comparison of caspase-7 activity before and after labeling (red bars). Upon Neutravidin affinity pull down, the probe-labeled caspase-7 was shown to retain most of its original activity (blue bars), indicating, even with covalent labeling, the enzyme still retained its catalytic activity. Wash-through fractions contained substantial caspase-7 activity, indicating most of the enzyme was not covalently modified. (D) QTOF MS determination of caspase-7 before and after labeling, indicating a majority of the protein was not covalently modified.

and -7 in cellular apoptosis, **P1** was selected as a candidate for further *in vitro* and *in vivo* studies. At optimized conditions (25 μM of **P1** with 1:20 caspase/**P1** ratio), the enzymatic reaction between **P1** and purified caspase-3/-7 was monitored in a time-dependent manner (Figure S2); typical saturation kinetics of enzymatic activity was observed. This demonstrated that fluorescence was dependent on catalytic cleavage of the substrate **WH**, Ac-DEVD, in **P1**, which spontaneously released the quencher. The fact that **P1** was acting like a typical fluorogenic protease substrate indicated that Pathway A (Figure 2A) was in operation and the majority of the released quinone methide intermediate was quenched by the bulk medium, that is, H_2O, and/or other nucleophiles present in the solution, such as DTT.[14b] We further determined the kinetic values of **P1** against caspase-3/-7 ($K_M = 31.99 \pm 0.13\ \mu$M and $k_{cat} = 7.1 \pm 0.1\ s^{-1}$ for caspase-3; $K_M = 69.83 \pm 0.11\ \mu$M and $k_{cat} = 5.0 \pm 0.3\ s^{-1}$ for caspase-7). In general, our probe has greater K_M and smaller k_{cat} values when compared to the commercial coumarin-based caspase-3/7 substrate Ac-DEVD-AFC (Table S2), giving approximately 10-fold lower catalytic efficiency (k_{cat}/K_M). This indicates our probe was multiply turned over and should serve as a reasonably efficient substrate for the enzymes. After reaching maximum fluorescence, the reaction mixtures were analyzed on a 20% SDS−PAGE gel followed by in-gel fluorescence scanning and staining with Coomassie blue (Figure 4B); two fluorescently labeled bands were observed, representing both the large (p17/p19) and small (p12/p11) subunits of active caspase-3/-7. This is presumably caused by covalent modification of the quinone methide intermediate (Pathway B in Figure 2A), a phenomenon often observed in previous studies.[13] Another significantly stronger fluorescent band, which co-migrated with the dye front, was also observed, but did not appear in the Coomassie gel. This band was subsequently identified to be the adduct of quinone methide-H_2O reaction (Pathway A). On the basis of the fluorescence/Coomassie gels, the labeled proteins were estimated to be <10% of total protein amount present in the reaction, thus, explaining the reason **P1**/caspase microplate assay followed typical enzyme kinetics. The microplate and labeling experiments were repeated with heat- and inhibitor-inactivated caspase-3/-7; neither fluorescence release nor protein labeling was observed, indicating both the substrate cleavage and enzyme labeling were activity-dependent. To more quantitatively assess the amount of labeled caspase and whether the labeled caspase still retains its enzymatic activity, one portion of the completed caspase-7/**P1** (1:20 ratio) reaction, as described above, was tested with Ac-DEVD-AFC (red bars in Figure 4C, and Figure S10); no significant decrease of caspase-7 activity was observed when compared with the untreated caspase-7 alone. The same reaction mixture was subjected to mass spectrometric (MS) analysis (Figure 4D); results indicated that most of the caspase-7 (>90%) in the reaction was not covalently labeled and showed an identical MS spectrum as the unmodified caspase-7. To further assess whether **P1**-labeled caspase-7 still retains its catalytic activity, the labeling mixture was affinity-enriched with Neutravidin beads, and washed until the flowthroughs were free of any caspase activity. Subsequent testing of the bead-bound (therefore covalently modified with **P1**) caspase-7 showed the enzyme still retained most of its catalytic activity (Figure 4C, blue bars). It is promising to observe that even probe-labeled protein adducts retained most of the enzymatic activity, enabling multiple turnovers of our qABP strategy.

In-Cell Bioimaging of Apoptosis Using qABPs. Next, we determined whether the strategy could be used for "imaging" enzyme localization in cells with sufficient sensitivity and spatial resolution. **P1** was again used as an example and its *in situ* labeling profiles against cellular lysates were analyzed by in-gel fluorescence scanning (Figure 5A). In both bacterial and apoptotic mammalian cell lysates, where caspase-3/-7 activities were overexpressed, the fluorescence labeling of caspase-3/-7 by **P1** was greatly diminished, while a wide number of nontarget proteins

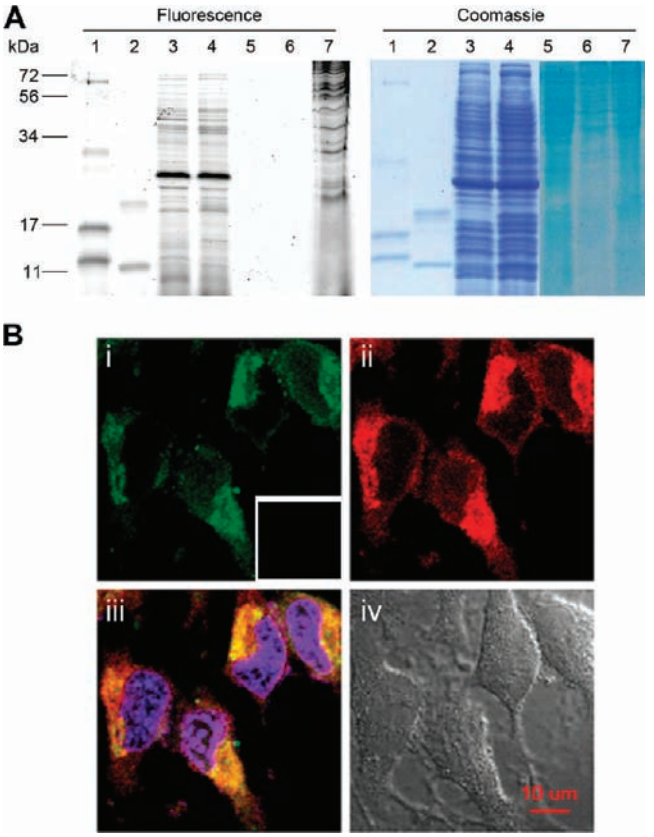

Figure 5. (A) *In vitro* labeling of **P1** in bacterial and mammalian lysates (free probe released from the reaction moved at the gel front and was not shown). Lanes 1 and 2, purified caspase-3 and -7; lanes 3 and 4, bacterial lysates overexpressing caspase-3 and -7; lane 5, bacterial lysate without inducing the overexpression of caspase-3/7; lane 6, normal HeLa cell lysate; lane 7, apoptotic HeLa cell lysate. (B) Confocal microscope images of caspase-3/-7 activities using **P1** in apoptotic HeLa cells and confirmed with immunofluorescence staining. Panel i: 488 nm channel (pseudocolored in green) detecting cellular localization of **P1**. (Inset) Normal HeLa cells incubated with **P1**. Panel ii: immunofluorescence staining at 543 nm channel (pseudocolored in red) using anti-caspase-3 primary antibody and anti-rabbit IgG-TR secondary antibody. Panel iii: merged images of panels I and ii, together with stained nuclei (with Hoechest; pseudocolored in blue). Panel iv: DIC image of the same cells. All images were acquired under the same settings. Scale bar = 10 μm. See Figure S13 for further details.

were clearly labeled (lanes 3, 4 and 7; compared to lanes 1 and 2). Some highly fluorescent free dye (e.g., the quinone methide-H_2O adduct) was also evident in these lanes but readily washed away with buffer (data not shown). Lysates of normal bacteria (nor expressing caspase-3/7) and HeLa cells did not show any significant fluorescent band upon incubation with **P1** (i.e., lane 5 and 6), nor did they release the free dye. These results demonstrate that Pathway C was indeed in operation as originally anticipated (Figure 2A); **P1**, upon activation by caspase-3/-7 in the cell lysates, released the reactive quinone methide intermediate which diffused away from the active site of the target (while keeping the enzyme active) and was subsequently "trapped" by other proteins in the vicinity. It should be pointed out that the very concept of using "reactive" chemical handles in a small molecule reporter to achieve localization near the site/organelle of the reaction is in fact not new, and has been extensively exploited in other commercial probes, that is, Mitrotracker.[4]

To determine whether these resultant, fluorescently labeled proteins could provide sufficient spatial resolution to accurately report localization of the enzyme target, confocal fluorescence microscopy was next used to image normal and apoptotic HeLa cells treated with **P1** (Figure 5B and Figure S13 in the Supporting Information). Owing to the relatively large size of our current probes (MW > 1000), they were not cell-permeable, but may be made so in the future by introducing a cell-penetrating peptide (vide infra).[16,17] So for most live cell experiments reported in this article, cells were first permeabilized by treatment of 1% digitonin (10% DMSO) for 1 min. Normal, un-induced cells showed an extremely low fluorescence signal (inset in Panel i, Figure 5B), indicative of little or no capase-3/-7 activity. Upon the addition of staurosporine (STS, an apoptosis trigger), an exponential increase of fluorescence signals was detected and spread throughout the cells. After washing off free dye and fixing the cells, strong green fluorescence signals were retained, which perfectly merged with Immunofluorescence (IF) signals generated from anti-caspase-3 primary antibody, which specifically detects both the large (17 kDa) and small (12 kDa) subunits of active Caspase-3, and a fluorescently labeled secondary antibody (Panels ii and iii). In contrast, no obvious fluorescence was detected when STS-induced cells were pretreated with a commercial caspase-3/-7 inhibitor, then **P1** (Figure S13), again highlighting that bioimaging of caspase-3/-7 activity in live mammalian cells with our probe was activity-dependent. The two control probes, **C1** and **C2**, were also used to image apoptotic HeLa cells under identical conditions (Figure S14); no significant fluorescence was observed for both probes. Taken together, we concluded that our qABPs were indeed suitable probes for live cell imaging of enzyme localization.

One- and Two-Photon qABPs for Tyrosine Phosphatases. To further expand the utility of our qABP strategy for *in vivo* imaging applications, two additional probes (**P5** and **P6**) with different dyes (one-photon and two-photon) were synthesized to target protein tyrosine phosphatases (PTPs) (Figure 2). Two-photon microscopy (TPM) provides key advantages over the usual one-photon imaging techniques, namely, increased penetration depth, lower tissue autofluorescence and self-absorption, and reduced photodamage and photobleaching.[3,23] The caged phosphate group was introduced to temporally control the detection of PTPs activities via an UV-mediated uncaging reaction.[19b] In the current study, we chose a simple photolabile 2-nitrobenzyloxy group as the caging molecule for synthetic convenience, but it may be readily replaced, if necessary, with other known two-photon caging molecules.[24] It was established that complete uncaging of probes **P5** and **P6** occurred with 1000 μJ/cm^2 UV exposure for 15 min (Figure S3). Using UV-irradiated probes, four different PTPs, including PTP1B, TCPTP, LMWPTP, and PTPB, were tested *in vitro* (Figures S4−S10); these PTP probes were found to work as expected with purified PTPs as well as PTP-expressing cell lysates. Furthermore, the photophysical properties of two-photon dye **22** and the corresponding 2-P probe, **P6**, before/after uncaging plus enzymatic treatment of PTPB in Hepes buffer were determined and summarized in Table 1. Upon uncaging and enzymatic treatment of PTPB, the two-photon action cross-section values ($\Phi\delta$) increased from 35 to 140 at 800 nm excitation, indicating a significant, definitive increase in the two-photon excited fluorescence (TPEF) intensity. In contrast, the $\Phi\delta$ value of **P5** was only 17 (Supporting Information), 8-fold lower than that of **P6**.

Table 1. Photophysical Properties of Dye 22, P6 before/after Uncaging and Treatment with PTPB in Hepes Buffer

compound	$\lambda_{max}^{(ab)a}$	$\varepsilon/10^3$	$\lambda_{max}^{(em)b}$	Φ^c	$\delta\Phi/GM^d$
Dye **22**	455	32	560	0.35	188
P6[e]	480	35	592	0.06	35
P6[f]	479	35	569	0.26	140

[a] Peak position of the longest absorption band. [b] Peak position of emission, exited at the absorption maximum. [c] Quantum yields determined by using fluorescein aqueous NaOH (pH = 13) as standard, respectively. [d] The maxima two-photon action cross-section values in GM (1 GM = $10^{-50}\cdot cm^4\cdot s\cdot photon^{-1}$) upon excitation from 750 to 860 nm. [e] **P6** before uncaging. [f] **P6** after uncaging and treatment with PTPB.

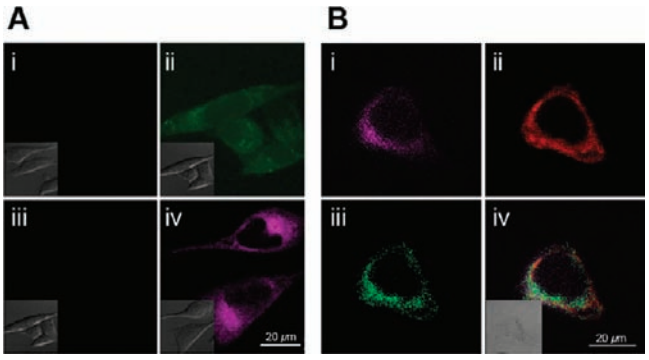

Figure 6. One and two-photon imaging using **P5** and **P6**. (A) Normal HeLa cells. Panel i: caged **P5** under one-photon excitation (488 nm). Panel ii: uncaged **P5** under one-photon excitation (488 nm). Panel iii: uncaged **P5** under two-photon excitation (800 nm). Panel iv: uncaged **P6** under two-photon excitation (800 nm). Scale bar = 20 μm. (B) PTP1B overexpressed HeLa cells (by transient transfection of pJ3H-PTP1B plasmid). Panel i: uncaged **P6** under two-photon excitation (800 nm). Panel ii: cells treated with ER tracker under one-photon excitation (543 nm). Panel iii: IF staining of PTP1B localization with mouse-anti-HA antibody (488 nm). Panel iv: merged images of i to iii. Scale bar = 20 μm. All images were acquired in the same way. (Inset) Corresponding DIC images. See Supporting Information for details.

Next, TPM was carried out to image endogenous PTP activities in HeLa cells (Figure 6A). Under one-photon excitation at 488 nm, cells treated with **P5** registered an increase in fluorescence upon UV irradiation (Panels i and ii). This clearly validates the temporal control of our probes in "turning-on" the detection only when needed. The fluorescence was observed throughout the cytosol of cells, indicating most endogenous PTP activities in HeLa cells were cytosolic. The same cells were imaged with TPM (excitation at 800 nm; Panel iii); no fluorescence was detected. In contrast, cells treated with **P6** exhibited strong fluorescence signals under the same conditions upon UV irradiation (Panel iv). Furthermore, it was observed that other fluorescence sources such as MitoTracker, LysoTracker and Hoechst were silent and background autofluorescence from the cells was negligible (data not shown). Images obtained under TPM were in general of better clarity and potentially offer higher resolution. All these lines of evidence clearly indicate the numerous advantages of TPM and our 2-P probes for *in vivo* enzyme imaging experiments in future applications. Finally, the commercial availability of an endoplasmic reticulum (ER)-localizing PTP1B construct enabled us to quickly and unambiguously confirm that our probes could indeed image localized enzyme activities within the cell (Figure 6B); HeLa cells transiently transfected with the pJ3H-PTP1B plasmid (which overexpresses and accumulates HA-tagged PTP1B in ER[25]), followed by imaging with **P6**, showed intense fluorescence only in ER (Panel i). Subsequent verifications were done with the ER tracker (Panel ii) and immunofluorescence staining of PTP1B (Panel iii). These results thus provide strong evidence that our probes were indeed successfully retained at the vicinity of targeted enzymes.

Live Cell Imaging with CPP-Containing Probe (P7). The relatively large size of our probes (MW > 1000) thus far necessitated the permeabilization of cells prior to imaging experiments. The modularity of our probe design, however, has enabled us to address this problem by the introduction of cell-penetrating peptides (CPP).[16,17] As shown in Figure 7A, the CPP-containing probe, **P7**, is similar to **P5** but contains an additional well-known CPP moiety of nine consecutive arginine residues (R_9).[17c,d] Similar to **P1**−**P6**, this probe was synthesized from the key intermediate **35** using solid-phase chemistry (Figure 2 and Scheme S4). With **P7** in hand, we next carried out bioimaging of endogenous PTP activities in live HeLa cells. As shown in Figure 7B, when **P7** was uncaged by UV irradiation prior to incubation with live HeLa cells, membrane-localized fluorescence was detected (Panel i), indicating that, upon reaching the cell membrane, the activated probe reacted with membrane-bound PTPs and was permanently "trapped". On the contrary, when **P7** was first incubated with live HeLa cells, then uncaged by UV irradiation, followed by imaging of PTP activities, most of the fluorescence signals were detected intracellularly (Panel ii), indicating the probe had been successfully delivered inside the live cells.

CONCLUSION

In conclusion, we have successfully developed a new class of "turn-on" qABPs suitable for the imaging of enzymatic activities in live mammalian cells, with sufficient spatial resolution and temporal control. The modular design of our probes based on quinone methide chemistry allows convenient introduction of different combinations of warheads and dyes (as well as other tags including CPP), thus, enabling the strategy to be generally applicable to a variety of enzymes and imaging techniques. One valuable feature of these new qABPs is that they do not inactivate the enzyme target, allowing amplification of the target signal *in situ*. We have demonstrated, for the first time, two-photon activity-based probes for live cell enzyme imaging. This new class of probes is thus expected to extend the repertoire of *in vivo* activity-based probes, opening up many new avenues for dissecting the biology of cells. Unlike other well-known organelle specific trackers such as Mitrotracker, which also make use of a reactive chemical handle to get "trapped" inside living cells,[4] the key difference in the current qABP design is that the quinone methide in our system will only be "turned-on" in the presence of the active target enzyme, thus, greatly reducing background fluorescence and improving specificity, and is also activity-based. While our manuscript was under review, Withers and co-workers reported what they call self-immobilizing fluorogenic imaging agents based on modified derivatives of coumarin glycosides for histological studies and fluorescence-activated cell sorting (FACS).[26] Coincidently, quinine methide was also used in their system to trap local glycosidase activities in live cells.

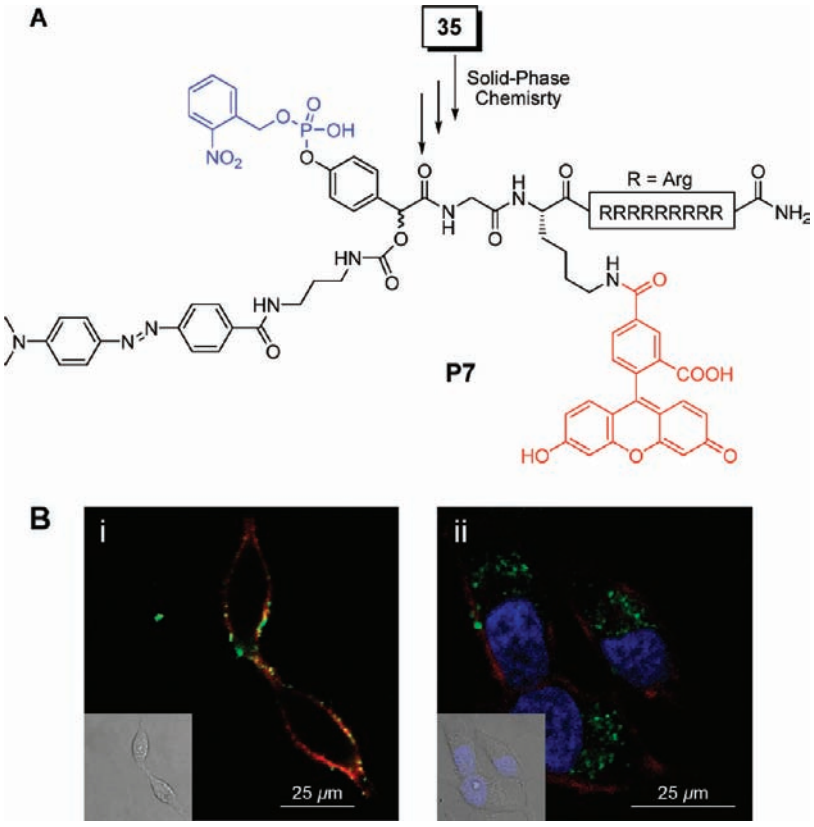

Figure 7. Live cell imaging of PTP activities using CPP-containing probe **P7**. (A) Structure of the cell-permeable **P7**. See Scheme S4 for detailed synthetic scheme. (B) Imaging of endogenous PTP activities using **P7**. Panel i: **P7** was uncaged prior to incubation with live HeLa cells. Fluorescence signals from **P7** (pseudocolored in green) and membrane tracker (pseudocolored in red) were merged. Panel ii: **P7** was incubated with live HeLa cells for 1 h, then uncaged, followed by imaging. Fluorescence signals from **P7** (pseudocolored in green), membrane tracker (pseudocolored in red), and nucleus staining (pseudocolored in blue) were merged. All images were acquired under same settings. Scale bar = 25 μm. See Figure S17 for details.

Albeit significantly different in both the design and chemical structure of probes, their studies provide further support to the utilities of our new qABPs. Finally, the biggest drawback of our first version of qABPs was arguably the lack of cell permeability (due to their relatively large size, i.e., MW > 1000). In the current study, we have been able to address this issue by simple attachment of CPPs, which was made possible due to the highly modular nature of our probe design. With our cell-permeable PTP probe, **P7**, which contains an R_9 cell-penetrating peptide, we had successfully detected localized PTP activities in live HeLa cells. We believe our probes may find wide applications in bioimaging of a variety of other endogenous enzymatic activities.

EXPERIMENTAL SECTION

General Information. The expression and purification of recombinant Caspase-3/-7 and PTPs (PTP1B, TCPTP, PTPB, LMWPTP) were carried out as previously reported.[27] Their enzymatic activities were routinely tested using the Caspase-3/7 substrate Ac-DEVD-AFC (Invitrogen) and general PTP substrate 6,8-difluoro-methyllumbeliferyl phosphate (Invitrogen). Other caspases, cathepsins, and legumain were obtained from commercial sources (EMD Merck and R&D System). The fluorogenic legumain substrate Z-AAN-AMC was obtained from Bachem, Switzerland. Antibodies were obtained from Abcam and Santa Cruz. Neutravidin beads were from Pierce. All other reagents were commercially available, unless otherwise indicated. The microplate enzymatic assays were carried out using a Synergy 4 microplate reader (Bioteck). In-gel fluorescence scanning of SDS−PAGE gels was carried out with a Typhoon 9410 fluorescence gel scanner (Amersham GE) equipped with a blue laser (488 nm) with suitable excitation/emission filters. The scanned images were quantified with the ImageQuant 3.3 software (Molecular Dynamics). All other experiments were carried out based on where they were described. UV−vis absorption/extinction and fluorescence spectra were measured with a Shimadzu UV−vis spectrophotometer and a Perkin-Elmer LS50 spectrofluorometer, respectively. The two-photon excitation fluorescence measurements were performed with a Spectra Physics femtosecond Ti:sapphire oscillator (Tsunami) as the excitation source. The output laser pulses have a tunable center wavelength from 750 to 860 nm with pulse duration of 40 fs and a repetition rate of 76 MHz. The laser beam was focused onto the samples that were contained in a cuvette with path length of 1 cm. The emission from the samples was collected at 90° angle by a pair of lenses and an optical fiber that was connected to a monochromator (Acton, Spectra Pro 2300i) coupled with CCD (Princeton Instruments, Pixis 100B) system. A short pass filter with cutoff wavelength at 700 nm was placed before the spectrometer to minimize the scattering from the pump beam. All the measurements were performed at room temperature. All one-photon cellular imaging results were taken with a LSM 510 Meta confocal microscope (Carl Zeiss, Germany) equipped with a plan-Apochromat 63×/1.40 Oil DIC objective, and the images were processed using the Zeiss LSM Image Browser (version: 4.2.0.121). All two-photon cellular imaging results were taken with a Leica TCS SP5X optical microscope system equipped with a Ti:Sapphire femtosecond laser and HCX PL APO 100×/1.40−0.70 OIL CS objective. All images were processed using the Leica image analysis software.

Chemical Synthesis. All chemicals were purchased from commercial vendors and used without further purification, unless indicated otherwise. Rink Amide resin, all Fmoc-protected amino acids, *O*-benzotriazole-*N*,*N*,*N*′,*N*′-tetramethyl-uronium-hexafluoro-phosphate (HBTU), *N*-hydroxybenzotriazole (HOBt), triisopropylsilane (TIS), and all other peptide synthesis reagents were purchased from GL Biochem (China). All nonaqueous reactions were carried out under a nitrogen atmosphere in oven-dried glassware. Reaction progress was monitored by TLC on precoated silica plates (Merck 60 F_{254}, 250 μm thickness) and spots were visualized by Ceric Ammonium Molybdate (CAM), basic $KMnO_4$, UV light or iodine. Flash column chromatography was carried out using Merck 60 F_{254} 0.040−0.063 μm silica gel. The ^{1}H and ^{13}C NMR spectra were taken on a Bruker 300 MHz or DPX-300 MHz or Bruker Avance 500 MHz NMR spectrometer. Chemical shifts are reported in parts per million (ppm) referenced with respect to residual solvent ($CDCl_3$ = 7.26 ppm, $(CD_3)_2SO$ = 2.50 ppm) or Tetramethylsilane ($Si(CH_3)_4$ = 0.00 ppm). ^{1}H NMR coupling constants (J) are reported in hertz (Hz) and the following abbreviations were used in reporting spectra: s = singlet, d = doublet, t = triplet, q = quartet, m = multiplet, dd = doublet of doublets, ddd = doublet of doublets of doublets, dt = doublet of triplets or overlap of nonequivalent resonances. Mass spectra were recorded on a Finnigan LCQ mass spectrometer, a Shimadzu LC-IT-TOF spectrometer or a Shimadzu LC-ESI spectrometer. Analytical HPLC was carried out on Shimadzu LC-IT-TOF or LC-ESI systems equipped with an autosampler, using reverse-phase Phenomenex Luna 5 μm C_{18} 100 Å 50 × 3.0 mm columns. Preparative HPLC was carried out on Gilson preparative HPLC system using Trilution software and reverse-phase Phenomenex Luna 5 μm $C_{18(2)}$ 100 Å 50 × 30.00 mm column. A 0.1% TFA/H_2O and 0.1% TFA/acetonitrile were used as eluents for all HPLC experiments. The flow rate was 0.6 mL/min for analytical HPLC and 10 mL/min for preparative HPLC. Details of synthetic procedures and characterizations of most compounds were reported in the Supporting Information. Characterizations of key intermediates and final probes are reported below.

(*E*)-9-(4-(2-(((9H-Fluoren-9-yl)methoxy)carbonylamino)-4-*tert*-butoxy-4-oxobutanamido)phenyl)-1-(4-((4-(dimethylamino)phenyl)diazenyl)phenyl)-1,7,10-trioxo-8-oxa-2,6,11-triazatridecan-13-oic Acid (17a). HPLC-grade THF was degassed with Argon for 1 h. Then compound **16a** (prepared from Fmoc-Asp(*t*Bu)−OH in multiple steps; see Scheme S2 in the Supporting Information) (2.4 g, 2.4 mmol) and $PhSiH_3$ (0.6 mL, 4.8 mmol) were added, followed by $Pd(PPh_3)_4$ (5 wt %, 120 mg) under an argon atmosphere. The reaction mixture was concentrated *in vacuo* and purified by flash chromatography (MeOH/DCM = 1:8) to afford **17a** as an orange compound (1.6 g, 69.2%). ^{1}H NMR (300 MHz, $CDCl_3$) δ 10.19 (s, 1H), 8.67 (s, 1H), 8.01 (d, J = 8.6 Hz, 2H), 7.88−7.79 (m, 7H), 7.70 (t, J = 7.2 Hz, 3H), 7.57 (t, J = 8.4 Hz, 3H), 7.38 (d, J = 7.2 Hz, 4H), 7.32−7.28 (m, 2H), 6.84 (d, J = 9.2 Hz, 2H), 5.82 (s, 1H), 4.51 (q, J = 7.9 Hz, 1H), 4.34−4.19 (m, 3H), 3.07 (s, 6H), 2.72 (m, 1H), 2.55 (m, 1H), 1.68 (t, J = 6.7 Hz, 2H), 1.36 (s, 9H). ^{13}C NMR (75 MHz, $CDCl_3$) δ 169.7, 169.53, 165.77, 155.46, 154.39, 153.30, 144.27, 144.19, 143.13, 141.17, 139.88, 139.29, 137.90, 135.26, 132.41, 129.40, 128.81, 128.31, 128.11, 127.77, 127.52, 125.73, 125.54, 121.96, 121.84, 120.55, 120.49, 119.68, 112.05, 110.20, 80.76, 74.90, 66.24, 52.68, 47.08, 38.69, 38.01, 37.42, 29.82, 28.23, 28.16. IT-TOF: m/z $[M + H]^+$ calcd 969.41, found 969.40.

9-(4-((*S*)-2-((((9H-Fluoren-9-yl)methoxy)carbonyl)amino)-4-carboxybutanamido)phenyl)-1-(4-((*E*)-(4-(dimethylamino)phenyl)diazenyl)phenyl)-1,7,10-trioxo-8-oxa-2,6,11-triazatridecan-13-oic Acid (17b). Obtained similarly from compound **16b** (prepared from Fmoc-Glu(*t*Bu)−OH as shown in Scheme S2). Yield: 61.8%. ^{1}H NMR (500 MHz, $CDCl_3$) δ 7.77 (s, 2H), 7.71 (s, 2H), 7.62 (s, 4H), 7.41 (s, 4H), 7.38−7.37 (d, J = 4.9 Hz, 2H), 7.26 (s, 4H), 7.15 (s, 2H), 6.62 (s, 2H), 4.29 (s, 2H), 4.15−4.07 (m, 4H), 2.98 (s, 6H), 2.30 (s, 2H), 2.15−2.09 (m, 2H), 1.58 (s, 2H), 1.34 (s, 9H). ^{13}C NMR (125 MHz, $CDCl_3$) δ 172.56, 156.56, 156.52, 154.74, 152.62, 143.79, 143.54, 141.09, 128.02, 127.53, 126.97, 125.29, 125.01, 122.03, 119.76, 111.38, 80.84, 67.16, 67.11, 66.31, 65.76, 60.46, 54.87, 49.86, 49.68, 49.52, 49.34, 46.92, 40.11, 35.14, 31.85, 31.51, 29.62, 29.29. IT-TOF: m/z $[M + H]^+$ calcd 983.42, found 983.41.

(*E*)-9-(4-(Bis(2-nitrobenzyloxy)phosphoryloxy)phenyl)-1-(4-((4-(dimethylamino)phenyl)diazenyl)phenyl)-1,7,10-trioxo-8-oxa-2,6,11-triazatridecan-13-oic Acid (35). Compound **34** (prepared based in Scheme S3 in the Supporting Information) (0.83 g, 0.86 mmol) and $PhSiH_3$ (0.2 mL, 1.7 mmol) dissolved in THF were added $Pd(PPh_3)_4$ (5 wt %, 41 mg) under an argon atmosphere. The reaction mixture was stirred for 30 min at room temperature before being concentrated *in vacuo* and purified by flash chromatography (MeOH/DCM = 1:8) to afford **35** as an orange product (0.63 g, 80%). ^{1}H NMR (300 MHz, $CDCl_3$) δ 8.64 (broad, NH), 8.11 (d, J = 3.8 Hz, 2H), 8.00 (d, J = 4.3 Hz, 2H), 7.81−7.73 (m, 6H), 7.65−7.59 (m, 4H), 7.52 (d, J = 4.3 Hz, 2H), 7.22 (d, J = 4.2 Hz, 2H), 6.82 (d, J = 4.6 Hz, 2H), 5.93 (s, 1H), 5.58 (d, J = 3.7 Hz, 4H), 3.68−3.53 (m, 4H), 3.30 (broad, 2H), 3.05 (s, 6H), 1.70 (t, J = 6.4 Hz, 2H). ^{13}C NMR (75 MHz, $CDCl_3$) δ 172.6, 167.9, 165.7, 154.9, 154.0, 152.8, 149.8, 149.7, 146.8, 142.7, 134.8, 134.4, 134.3, 129.6, 129.6, 128.8, 128.3, 125.1, 124.9, 121.5, 119.92, 119.86, 111.5, 73.8, 66.4, 66.3, 38.3, 37.0, 29.4. ^{31}P NMR (121 MHz, MeOD) δ −6.15. IT-TOF: m/z $[M + H]^+$ calcd 927.26, found 927.26.

Synthesis, Purification, and Characterizations of the Protease Probes (P1−P4, C1, and C2) and the PTP Probes (P5−P7). First, Fmoc-Lys(Biotin)−OH (4 equiv) was synthesized following previously published procedures.[28] To load it onto rink amide AM resin, it was dissolved in dry DMF (1.5 mL) together with HBTU (4 equiv), HOBt (4 equiv), and DIEA (8 equiv). The resin (50 mg, loading ∼0.5 mmol/g, premixed in dry DMF) was added and the resulting mixture was shaken for 3 h at room temperature. The resin was filtered and washed thoroughly with DMF (3×), DCM (3×), and DMF (3×) until the filtrate became colorless. Any unreacted resin was capped with a solution of Ac_2O (10 equiv), DIEA (20 equiv) in DCM, and the reaction mixture was allowed to react for 2 h at room temperature, followed by extensive washes with DCM (3×) and DMF (3×). Next, the Fmoc-protected amino-functionalized resin was treated with 20% piperidine in DMF for 1 h at room temperature, then washed with DMF (3×), DCM (3×), and DMF (3×). The coupling of an Fmoc-protected amino acid was carried out using the following general procedure. Fmoc-amino acid (4 equiv), HBTU (4 equiv), and HOBt (4 equiv) were dissolved in dry DMF (1.5 mL) and DIEA (8 equiv) was added and agitated for 5 min. This preactivated Fmoc-amino acid solution was added to the resin and shaking was continued for 3 h at room temperature. The resin was filtered and washed with DMF (3×), DCM (3×), and DMF (3×). To couple **17a** and **17b**, the compound (4 equiv), HATU (4 equiv), and HOAt (4 equiv) were dissolved in dry DMF (1.5 mL). DIEA (8 equiv) was added and the resulting mixture was agitated for 5 min. This preactivated unnatural amino acid solution was added to the resin and shaking was continued overnight at room temperature. The resin was filtered and washed with DMF (3×), DCM (3×), and DMF (3×). The procedure for the coupling of Fluorescein-(OAc)-NHS (step **g** in Scheme S2) was the following. First, the resin was swollen in dry DCM for 30 min, then treated with 1% TFA, 5% TIS in DCM (1.5 mL) for another 30 min. Successful Mtt deprotection was indicated by ninhydrin test. The resin was washed with DMF (3×), DCM (3×) and DMF (3×), then added into an DMF solution containing Fluorescein(OAc)-NHS (4 equiv) and DIEA (8 equiv) (1.5 mL) followed by shaking overnight at room temperature. The resin was filtered, then washed with DMF (3×), DCM (3×), and DMF (3×), followed by capping with with Ac_2O (10 equiv) and DIEA (20 equiv) in DCM for 2 h

at room temperature. Upon washing with DCM (3×) and DMF (3×), the resin was treated with 20% piperidine in DMF (10 min) to remove the acetyl group, giving free fluorescein. To cleave the final probe from the solid support, the resin was washed with MeOH (3×) and dried thoroughly *in vacuo*. A solution of TFA/TIS/H_2O (95/2.5/2.5; 2 mL) was added and the mixture was shaken at room temperature for 2.5 h. The resin was filtered and washed with DCM (2×). The combined filtrate and DCM solutions were concentrated to ~0.5 mL, then precipitated by addition of cold diethyl ether (5 mL). The precipated peptide was collected by centrifugation, washed with cold diethyl ether twice, and dried *in vacuo*. The crude peptide was dissolved in DMSO and purified by Prep-HPLC using eluents A (0.1% TFA/water) and B (0.1% TFA/acetonitrile) from 10% B to 70% B in 35 min. Fractions containing the product were collected, concentrated, and lyophilized to give the final pure probe in the form of a solid. Normally, the probe was made to 10 mM stock in DMSO and kept at −20 °C freezer until use. Each probe was characterized by LC−MS to ensure its positive ID and homogeneity.

P1 (Ac-DEVD) IT-TOF-MS: exact ms calcd, 2028.80; found, 1015.86 $[(M + 2H)/2]^+$

P2 (Ac-YVAD) IT-TOF-MS: exact ms calcd, 2018.83; found, 1010.36 $[(M + 2H)/2]^+$

P3 (Ac-LEVD) IT-TOF-MS: exact ms calcd, 2026.86 found, 1014.90 $[(M + 2H)/2]^+$

P4 (Ac-VEID) IT-TOF-MS: exact ms calcd, 2026.86; found, 1014.90 $[(M + 2H)/2]^+$

C1 (Ac-D) IT-TOF-MS: exact ms calcd, 1685.66; found, 843.84 $[(M + 2H)/2]^+$

C2 (Ac-E) IT-TOF-MS: exact ms calcd, 1699.68; found, 851.31 $[(M + 2H)/2]^+$

To a solution of **35** (0.17 g, 0.18 mmol) in dry DMF was added **27** (prepared based in Scheme S3 in the Supporting Information) (0.13 g, 0.25 mmol), HATU (87 mg, 0.23 mmol), and DIEA (0.04 mL, 0.22 mmol). The reaction mixture was stirred at room temperature for 6 h. Upon removal of DMF, the residue was purified directly by Prep-HPLC to obtain **P5** (8.9 mg; 3.8% after Prep HPLC). Similarly, the precursor **24** (prepared based on Scheme S3) (70 mg, 0.1 mmol was used to prepare the probe **P6** (7.6 mg; 7.6% after Prer-HPLC). P7 was similarly synthesized from the key intermediate **35**, following solid-phase chemistry (Scheme S4), from a Rink amide resin preloaded with the R_9 sequence. LC−MS was used, as previously described, to characterize the compounds.

P5 (1-P PTP) IT-TOF-MS: exact ms calcd, 1340.39; found, 1341.37 $[M + H]^+$

P6 (2-P PTP) IT-TOF-MS: exact ms calcd, 1492.64; found, 1493.64 $[M + H]^+$

P7 IT-TOF-MS: exact ms calcd, 2682.86; found, 895.41 $[(M + 3H)/3]^+$

Microplate Enzyme Assay with P1−P6. Ten millimolar DMSO stock solutions of **P1** and **P2**−**P4** were diluted with Caspase-3/7 Assay Buffer (50 mM PIPES, 100 mM NaCl, 1 mM EDTA, 0.1% w/v CHAPS, 25% w/v sucrose, pH = 7.2) and PBS buffer, respectively, to make 10 μM working solutions. **C1** and **C2** (negative control probes) were similarly diluted with PBS buffer. Ten millimolar DMSO stocks of **P5** and **P6** were diluted with Hepes buffer (25 mM HEPES, 0.05 M NaCl, 2.5 mM EDTA, 2 mM DTT, 0.02% Triton X-100, pH = 7.5) to give 40 μM working solutions, then exposed under UV to uncage the phosphate group. The recombinant Caspase-3 and -7 were freshly diluted to ~0.02 μg/μL using Caspase-3/7 Assay Buffer containing 5 mM TCEP. Other commercial caspases and cathepsins were used following protocols provided by the vendor. Recombinant PTPs were freshly prepared in the Hepes buffer to ~0.1 μg/μL concentration. Legumain was freshly diluted to 100 μg/mL in activation buffer (50 mM sodium acetate, 100 mM NaCl, pH = 4.0) and incubated for 2 h at 37 °C followed by further dilution to 0.01 μg/μL in assay buffer (50 mM MES, 250 mM NaCl, pH = 5.0). In a typical enzymatic reaction, 10 μL of each probe (for positive controls, a commercially available fluorogenic substrate was used) was mixed with 10 μL of the enzyme solution and the reaction was continuously monitored at room temperature. Results are reported in Figure 4A and Figures S2−S7 (Supporting Information).

Activities of Probe-Labeled Enzymes. The enzyme (0.2 and 1 μg for caspase and PTP, respectively) was first incubated with the probe (5 and 20 μM of **P1** and uncaged **P5**, respectively) for 1 h. Subsequently, 4 μM (final concentration) of the fluorogenic enzyme substrate (Ac-DEVD-AFC and DiFMUP, respectively) was added. Independently, an identical reaction with enzyme and substrate ONLY was prepared. Both reactions were concurrently monitored continuously with the Synergy 4 microplate reader for at least 1 h (Figure S10). In a separate experiment, covalently labeled enzyme from above labeling reaction was affinity-separated from unlabeled enzyme, and their enzymatic activity was compared.[29] Briefly, 20 μg of recombinant Caspase-7 was incubated with **P1** (10 nmol giving 1:20 caspase/**P1** molar ratio) for 3 h. Subsequently, Neutravidin beads were added and the reaction was further incubated for 30 min at room temperature. A control pull-down experiment was carried out under exact conditions with the same amount of unlabeled Caspase-7 and Neutravidin beads. The beads were washed extensively with deionized water until no Caspase-7 activity was observed in the eluent. The Caspase-7 activity bound to the beads was tested using substrate Ac-DEVD-AFC (4 μM final concentration). Our results confirmed that most of the enzyme was not covalently labeled (despite excessive amount of probe used), and the probe-labeled enzyme still retained most of its catalytic activity (Figure 4C).

Mass Spectrometry. Twenty micrograms of Caspase-7 was labeled as above-described (1:20 caspase/**P1** molar ratio) overnight at room temperature. The sample, together with another control sample of unlabeled Caspase-7, was purified using a C_4 Ziptip (Millipore) according to manufacturer's instructions. Purified samples were eluted using 60% acetonitrile (in water) containing 0.1% formic acid. The samples were analyzed with a quadrupole time-of-flight QTOF Premier mass spectrometer (Waters, U.K.) equipped with a nanoelectrospray ion source. The protein molecular weight was acquired using lysozyme as an internal standard. As shown in Figure 4D, most of the caspase (>90%) in the labeling reaction was not covalently modified.

Gel-Based Labeling Experiments. Both stock solutions of **P1** and **P5** were prepared as described above and used for labeling with recombinant caspases/PTPs and lysates, respectively. For labeling with recombinant proteins, around 1 μg of each protein was incubated with the corresponding probe (**P1**, 25 μM final probe concentration giving 1:20 caspase/**P1** molar ratio; **P5**, 40 μM final probe concentration giving 1:40 PTP/**P5** molar ratio) at room temperature for 3 h. For lysates labeling, bacterial and mammalian lysates were prepared as described previously and below.[5c,27a,30] Bacteria transformed with a caspase-3/7 expressing plasmid was used. For bacterial lysates, upon induction of caspase expression and further growth, cells were collected and lysed to obtain the corresponding lysates. For mammalian lysate labeling, HeLa cells were cultured in DMEM growth media supplemented with 10% FBS and 1% penstrep. Cells were grown to a confluency of around 90% at 37 °C and 5% CO_2 in a humidified incubation chamber, followed by treatment with 1 μM staurosporine (STS) for 6 h to induce apoptosis.[5c] The cell pellets were harvested and lysed in PBS buffer with 6% glycerol. The supernatant was obtained by centrifugation at 13 000 rpm for 40 min at 4 °C. The amount of total proteins in the lysate was determined using the Bradford assay according to manufacturer's protocol. Caspase activities in both bacterial and mammalian lysates were confirmed using a Caspase-3/7 substrate (Ac-DEVD-AFC) as well as Western blotting according to the protocol provided by the vendor. In a labeling reaction, 30 μg (in protein content) of each lysate was

incubated with 5 μM of **P1** or uncaged **P5**, respectively, at room temperature for 3 h. All labeling reactions were stopped by addition of 6× SDS loading dye, followed by heating at 95 °C for 10 min. The mixture was resolved on a 12% or 20% SDS−PAGE gel and fluorescently labeled bands were visualized by in-gel fluorescence scanning. Coomassie blue staining and/or Western blotting (using anti-Caspase-3/7 antibodies; see Figure S12A,B in the Supporting Information) were carried out, where applicable. In some cases, 2D-PAGE was carried out (Figure S12C).

Cellular Imaging. HeLa cells were cultured as above-described. Subsequently, cells were permeabilized by treatment with 1% digitonin (in 10% DMSO) for 1 min and washed with PBS buffer (3×). **P1** (33.3 μM final conc.; with or without an inhibitor), **P5**, or **P6** (20 μM final conc.), prediluted with phenol-red free DMEM, was subsequently added. After 30 min, 500 nM of STS was added to induce apoptosis (for **P1** imaging only). Cells were further incubated for another 1.5 h and washed with PBS buffer (3×). For **P5**/**P6** imaging, cells were subsequently UV-iradiated (1000 μJ/cm^2) for 10 min. Nucleus was stained with Hoechest stain. To fix the cells, 4% formaldehyde was applied for 30 min, and cells were washed with PBS, then treated with 1% BSA in PBS buffer (to quench free aldehyde and block nonspecific binding), before application of primary and secondary antibodies (anti-rabbit IgG-TR), prepared in PBS buffer containing 1% BSA according to protocols from the vendor. Upon further incubation and washing with PBS buffer, cells were imaged. One- and two-photon imaging was carried out using HeLa cells, similar to what was described above. For live-cell imaging using **P7**, cells were directly treated with the probe without any permeabilization steps.

Transfection. The pJ3H-PTP1B plasmid, which expresses PTP1B with an HA tag, was purchased from Addgene, and transiently transfected into HeLa cells (at 90% confluence) with Lipofectamine 2000 reagent (Invitrogen), as previously described.[31] After proteins were expressed, cells were permeabilized and incubated with **P6** for 1 h. Nontransfected cells were used as negative controls. Subsequently, cells were fixed and blocked with 2% BSA in PBS for 30 min at room temperature, washed twice with PBS, then further incubated with mouse anti-HA primary antibody (Roche, 1:200) for 1 h at room temperature, and with FITC-conjugated anti-mouse IgG (Santa Cruz, 1:500) for 1 h, then imaged. For co-localization experiments, cells were further incubated with ER-Tracker Red (Invitrogen) for 1 h at room temperature, washed, and then imaged. All images were taken under similar conditions.

■ ASSOCIATED CONTENT

Supporting Information. Other relevant experimental section and synthetic procedures, spectral characterization of new compounds, and supplementary biological screening results. This material is available free of charge via the Internet at http://pubs.acs.org.

■ AUTHOR INFORMATION

Corresponding Author
chmyaosq@nus.edu.sg

■ ACKNOWLEDGMENT

Financial support was provided by the Ministry of Education (R-143-000-394-112), the Agency for Science, Technology and Research (R-143-000-391-305). The authors thank Dr. Yong Xiao and Yan Tong for technical support on two-photon microscope, and Jigang Wang for 2D and MS experiments.

■ REFERENCES

(1) (a) Tsien, R. Y. *Angew. Chem., Int. Ed.* **2009**, *48*, 5612–5626. (b) Fernandez-Suarez, M.; Ting, A. Y. *Nat. Rev. Mol. Cell Biol.* **2008**, *9*, 929–943. (c) Wang, H.; Nakata, E.; Hamachi, I. *ChemBioChem* **2009**, *10*, 2560–2577. (d) Biju, V.; Itoh, T.; Ishikawa, M. *Chem. Soc. Rev.* **2010**, *39*, 3031–3056. (e) Terai, T.; Nagano, T. *Curr. Opin. Chem. Biol.* **2008**, *12*, 515–521. (f) Domaille, D. W.; Que, E. L.; Chang, C. J. *Nat. Chem. Biol.* **2008**, *4*, 168–175.

(2) Zhang, J.; Campbell, R. E.; Ting, A. Y.; Tsien, R. Y. *Nat. Rev. Mol. Cell Biol.* **2002**, *3*, 906–918.

(3) (a) Wang, X.; Nguyen, D. M.; Yanez, C. O.; Ahn, H. Y.; Bondar, M. V.; Belfield, K. D. *J. Am. Chem. Soc.* **2010**, *132*, 2237–12239. (b) Kim, H. J.; Han, J. H.; Kim, M. K.; Lim, C. S.; Kim, H. M.; Cho, B. R. *Angew. Chem., Int. Ed.* **2010**, *49*, 6786−6789 and references cited therein.

(4) Invitrogen Home Page. www.invitrogen.com.

(5) (a) Edgington, L. E.; Berger, A. B.; Blum, G.; Albrow, V. E.; Paulick, M. G.; Lineberry, N.; Bogyo, M. *Nat. Med.* **2009**, *15*, 967–973. (b) Pratt, M. R.; Sekedat, M. D.; Chiang, K. P.; Muir, T. W. *Chem. Biol.* **2009**, *16*, 1001–1012. (c) Li, J.; Yao, S. Q. *Org. Lett.* **2009**, *11*, 405–408. (d) Watzke, A.; Kosec, G.; Kindermann, M.; Jeske, V.; Nestler, H. P.; Turk, V.; Turk, B.; Wendt, K. U. *Angew. Chem., Int. Ed.* **2008**, *47*, 406–409.

(6) Baruch, A.; Jeffery, D. A.; Bogyo, M. *Trends Cell Biol.* **2004**, *14*, 29−35 and references cited therein.

(7) (a) Blum, G.; Mullins, S. R.; Keren, K.; Fonovic, M.; Jedeszko, C.; Rice, M. J.; Sloane, B. F.; Bogyo, M. *Nat. Chem. Biol.* **2005**, *1*, 203–209. (b) Blum, G.; von Degenfeld, G.; Merchant, M. J.; Blau, H. M.; Bogyo, M. *Nat. Chem. Biol.* **2007**, *3*, 668–677.

(8) Aye-Han, N. N.; Li, Q.; Zhang, J. *Curr. Opin. Chem. Biol.* **2009**, *13*, 392–397.

(9) Zhang, X.-B.; Waibel, M.; Hasserodt, J. *Chem.—Eur. J.* **2010**, *16*, 792–795.

(10) For general reviews on small molecule activity-based probes (ABPs), see (a) Evans, M. J.; Cravatt, B. F. *Chem. Rev.* **2006**, *106*, 3279–3301. (b) Sadaghiani, A. M.; Verhelst, S. H. L.; Bogyo, M. *Curr. Opin. Chem. Biol.* **2007**, *11*, 20–28. (c) Uttamchandani, M.; Li, J.; Sun, H.; Yao, S. Q. *ChemBioChem* **2008**, *9*, 667–675.

(11) Blum, G.; Weimer, R. M.; Edgington, L. E.; Adams, W.; Bogyo, M. *PLoS One* **2009**, *4*, e6374.

(12) (a) Weinert, E. E.; Dondi, R.; Colloredo-Melz, S.; Frankenfield, K. N.; Mitchell, C. H.; Freccero, M.; Rokita, S. E. *J. Am. Chem. Soc.* **2006**, *128*, 1940–1947. (b) Sellars, J. D.; Landrum, M.; Congreve, A.; Dixon, D. P.; Mosely, J. A.; Beeby, A.; Edwards, R.; Steel, P. G. *Org. Biomol. Chem.* **2010**, *8*, 1610–1618.

(13) (a) Lo, L.-C.; Pang, T. L.; Kuo, C. H.; Chiang, Y. L.; Wang, H. Y.; Lin, J. J. *J. Proteome Res.* **2002**, *1*, 35–40. (b) Zhu, Q.; Girish, A.; Chattopadhaya, S.; Yao, S. Q. *Chem. Commun.* **2004**, 1512–1513. (c) Srinivasan, R.; Huang, X.; Ng, S. L.; Yao, S. Q. *ChemBioChem* **2006**, *7*, 32–36. (d) Komatsu, T.; Kikuchi, K.; Takakusa, H.; Hanaoka, K.; Ueno, T.; Kamiya, M.; Urano, Y.; Nagano, T. *J. Am. Chem. Soc.* **2006**, *128*, 15946–15947. (e) Blais, D. R.; Brûlotte, M.; Qian, Y.; Bélanger, S.; Yao, S. Q.; Pezacki, J. P. *J. Proteome Res.* **2010**, *9*, 912–923.

(14) (a) Lo, L.-C.; Lo, C.-H. L.; Janda, K. D. *Bioorg. Med. Chem. Lett.* **1996**, *6*, 2117–2120. (b) Lo, L.-C.; Chiang, Y. L.; Kuo, C. H.; Liao, H. K.; Chen, Y. J.; Lin, J. J. *Biochem. Biophys. Res. Commun.* **2005**, *326*, 30–35.

(15) Cravatt, B. F.; Wright, A. T.; Kozarich, J. W. *Annu. Rev. Biochem.* **2008**, *77*, 383–414.

(16) Lee, M. R.; Baek, K. H.; Jin, H. J.; Jung, Y. G.; Shin, I. *Angew. Chem., Int. Ed.* **2004**, *43*, 1675–1678.

(17) (a) Loh, Y.; Shi, H.; Hu, M.; Yao, S. Q. *Chem. Commun.* **2010**, *46*, 8407–8409. (b) Rajendran, L.; Knolker, H. J.; Simons, K. *Nat. Rev. Drug Discovery* **2010**, *9*, 29–42. (c) Stewart, K. M.; Horton, K. L.; Kelley, S. O. *Org. Biomol. Chem.* **2008**, *6*, 2242–2255. (d) Futaki, S. *Biopolymers* **2006**, *84*, 241–249.

(18) Thornberry, N. A.; Rano, T. A.; Peterson, E. P.; Rasperi, D. M.; Timkey, T.; Garcia-Calvo, M.; Houtzageri, V. M.; Nordstromi, P. A.; Royi, S.; Vaillancourti, J. P.; Chapman, K. T.; Nicholson, D. W. *J. Biol. Chem.* **1997**, *272*, 17907–17911.

(19) (a) Mayer, G.; Heckel, A. *Angew. Chem., Int. Ed.* **2006**, *45*, 4900–4921. (b) Rothman, D. M.; Vazquez, E. M.; Vogel, E. M.; Imperiali, B. *Org. Lett.* **2002**, 865–868.

(20) Kato, D.; Boatright, K. M.; Berger, A. B.; Nazif, T.; Blum, G.; Ryan, C.; Chehade, K. A. H.; Salvesen, G. S.; Bogyo, M. *Nat. Chem. Biol.* **2005**, *1*, 33–38.

(21) Manoury, B.; Hewitt, E. W.; Morrice, N.; Dando, P. M.; Barrett, A. J.; Watts, C. *Nature* **1998**, *396*, 695–699.

(22) All recombinant enzymes were tested with the commercial fluorogenic substrates to ensure they are catalytically active under our assay conditions. For example, legumain was routinely tested with Z-AAN-AMC substrate. For other enzymes, see Experimental Section for details.

(23) (a) Kim, H. M; Cho, B. R. *Chem. Commun.* **2009**, 153–164. (b) Pawlicki, M.; Collins, H. A.; Denning, R. G.; Anderson, H. L. *Angew. Chem., Int. Ed.* **2009**, *48*, 3244–3266. (c) He, G. S.; Tan, L.−S.; Zheng, Q.; Prasad, P. N. *Chem. Rev.* **2008**, *108*, 1245–1330.

(24) (a) Neveu, P.; Aujard, I.; Benbrahim, C.; Le Saux, T.; Allemand, J.-F.; Vriz, S.; Bensimon, D.; Jullien, L. *Angew. Chem., Int. Ed.* **2008**, *47*, 3744–3746. (b) Zhu, Y.; Pavlos, C. M.; Toscano, J. P.; Dore, T. M. *J. Am. Chem. Soc.* **2006**, *128*, 4267–4276.

(25) Rhee, J.; Lilien, J.; Balsamo, J. *J. Biol. Chem.* **2001**, *276*, 6640–6644.

(26) Kwan, D. H.; Chen, H.−M.; Ratananikom, K.; Hancock, S. M.; Watanabe, Y.; Kongsaeree, P. T.; Samuels, A. L.; Withers, S. G. *Angew. Chem., Int. Ed.* **2011**, *50*, 300–303.

(27) (a) Ng, S. L.; Yang, P.-Y.; Chen, K. Y.-T.; Srinivasan, R.; Yao, S. Q. *Org. Biomol. Chem.* **2008**, *6*, 844–847. (b) Yang, P.-Y.; Wu, H.; Lee, M. Y.; Xu, A.; Srinivasan, R.; Yao, S. Q. *Org. Lett.* **2008**, *10*, 1881–1884. (c) Tan, L. P.; Wu, H.; Yang, P.-Y.; Kalesh, K. A.; Zhang, X.; Hu, M.; Srinivasan, R.; Yao, S. Q. *Org. Lett.* **2009**, *11*, 5102–5105.

(28) (a) Uttamchandani, M.; Wang, J.; Li, J.; Hu, M.; Sun, H.; Chen, K. Y.-T.; Liu, K.; Yao, S. Q. *J. Am. Chem. Soc.* **2007**, *129*, 7848–7858.

(29) Lue, R. Y. P.; Chen, G. Y. J.; Hu, Y.; Zhu, Q.; Yao, S. Q. *J. Am. Chem. Soc.* **2004**, *126*, 1055–1062.

(30) Wu, H.; Ge, J.; Yang, P.-Y.; Wang, J.; Uttamchandani, M.; Yao, S. Q. *J. Am. Chem. Soc.* **2011**, *133*, 1946–1954.

(31) Yang, P.-Y.; Liu, K.; Ngai, M. H.; Lear, M. J.; Wenk, M.; Yao, S. Q. *J. Am. Chem. Soc.* **2010**, *132*, 656–666.